JB Journals.ASM.org

Characterization of Two UDP-Gal:GalNAc-Diphosphate-Lipid β1,3-Galactosyltransferases WbwC from *Escherichia coli* Serotypes O104 and O5

Shuo Wang,[a] Diana Czuchry,[a] Bin Liu,[b] Anna N. Vinnikova,[a] Yin Gao,[a] Jason Z. Vlahakis,[c] Walter A. Szarek,[c] Lei Wang,[b] Lu Feng,[b] Inka Brockhausen[a]

Department of Medicine and Department of Biomedical and Molecular Sciences, Queen's University, Kingston, Ontario, Canada[a]; TEDA School of Biological Sciences and Biotechnology, Nankai University, Tianjin, China[b]; Department of Chemistry, Queen's University, Kingston, Ontario, Canada[c]

***Escherichia coli* displays O antigens on the outer membrane that play an important role in bacterial interactions with the environment. The O antigens of enterohemorrhagic *E. coli* O104 and O5 contain a Galβ1-3GalNAc disaccharide at the reducing end of the repeating unit. Several other O antigens contain this disaccharide, which is identical to the mammalian O-glycan core 1 or the cancer-associated Thomsen-Friedenreich (TF) antigen. We identified the *wbwC* genes responsible for the synthesis of the disaccharide in *E. coli* serotypes O104 and O5. To functionally characterize WbwC, an acceptor substrate analog, GalNAcα-diphosphate-phenylundecyl, was synthesized. WbwC reaction products were isolated by high-pressure liquid chromatography and analyzed by mass spectrometry, nuclear magnetic resonance, galactosidase and O-glycanase digestion, and anti-TF antibody. The results clearly showed that the Galβ1-3GalNAcα linkage was synthesized, confirming $WbwC_{ECO104}$ and $WbwC_{ECO5}$ as UDP-Gal:GalNAcα-diphosphate-lipid β1,3-Gal-transferases. Sequence analysis revealed a conserved DxDD motif, and mutagenesis showed the importance of these Asp residues in catalysis. The purified enzymes require divalent cations (Mn^{2+}) for activity and are specific for UDP-Gal and GalNAc-diphosphate lipid substrates. WbwC was inhibited by bis-imidazolium salts having aliphatic chains of 18 to 22 carbons. This work will help to elucidate mechanisms of polysaccharide synthesis in pathogenic bacteria and provide technology for vaccine synthesis.**

The O antigens of lipopolysaccharides (LPS) in Gram-negative bacteria consist of many repeats of a specific oligosaccharide unit and are a major contributor to the antigenic variability of the bacterial cell surface, conferring defense to the bacteria against host killing mechanisms (1–5).

The O antigen gene clusters contain the corresponding glycosyltransferase (GT) genes, most of which have not yet been biochemically characterized. These GTs are likely to be responsible for completing the synthesis of the O antigen repeating unit by adding sugars to the nonreducing end of the oligosaccharide (6, 7). The repeating units are thought to be preassembled on the cytosolic face of the inner membrane, where the catalytic domains of GTs are directed into the cytoplasm with access to the nucleotide sugar donor substrate pools, as well as to the membrane-bound undecaprenol-phosphate (P-Und)-linked acceptor substrates (8, 9).

E. coli strains O104 and O5 produce Shiga toxins (10), which are known to cause severe bloody diarrhea in humans, sometimes leading to hemolytic uremic syndrome and death (11, 12). Shiga toxin-producing *E. coli* O104 (STEC) has acquired a second gene encoding a Shiga toxin variant (13). Several outbreaks of O104 infections have been reported worldwide (12); for example, an outbreak occurred in 2011 in Germany, in which thousands were infected, 53 people died, and many still suffer from the consequences of infections. In light of growing worldwide antibiotic resistance, alternative therapies such as immune therapies become more important. *E. coli* O104 synthesizes an O antigen with a tetrasaccharide repeating-unit structure of (-4-D-Galα1-4Neu5,7,9Ac_3α2-3-D-Galβ1-3-D-GalNAcβ1-)$_n$ (14), which could be the basis for a vaccine. The O5 antigen has the repeating-unit structure (4-D-Qui*p*3NAcβ1-3-D-Rib*f*β1-4-D-Gal*p*β1-3-D-GalNAcα1-)$_n$ (15). Thus, the two O antigens share the Galβ1-3GalNAcα disaccharide sequence, which is identical to O-glycan core 1 of mammalian glycoproteins and the cancer-associated Thomsen-Friedenreich (TF) antigen (16, 17). The genes of the O104 antigen gene cluster include three putative glycosyltransferase genes, *wbwA*, *wbwB*, and *wbwC*, in addition to CMP-NeuNAc synthesis genes, the O antigen polymerase *wzy* gene, and a flippase *wzx* gene (18). This suggests that O104 antigen synthesis follows the Wzy-dependent pathway. Since the *wbwC* gene from *E. coli* O104 has 44% identity to the *orf11* gene from *E. coli* O5, we propose that these genes encode orthologous enzymes that synthesize the Galβ1-3GalNAcα linkage.

The assembly of the O104 and O5 antigen repeating units is thought to be initiated by the transfer of GalNAcα-phosphate to undecaprenol-phosphate (P-Und) by the membrane-bound enzyme GlcNAc/GalNAc-phosphotransferase WecA (see Fig. S1 in the supplemental material). Alternatively, GlcNAcα-phosphate may be transferred, followed by 4-epimerization of GlcNAc (19) to form the acceptor substrate for WbwC, GalNAcα-PP-Und. Membrane-associated GTs then transfer sugar residues from

Received 7 April 2014 Accepted 12 June 2014

Published ahead of print 23 June 2014

Address correspondence to Lu Feng, fenglu63@nankai.edu.cn, or Inka Brockhausen, brockhau@queensu.ca.

Supplemental material for this article may be found at http://dx.doi.org/10.1128/JB.01698-14.

doi:10.1128/JB.01698-14

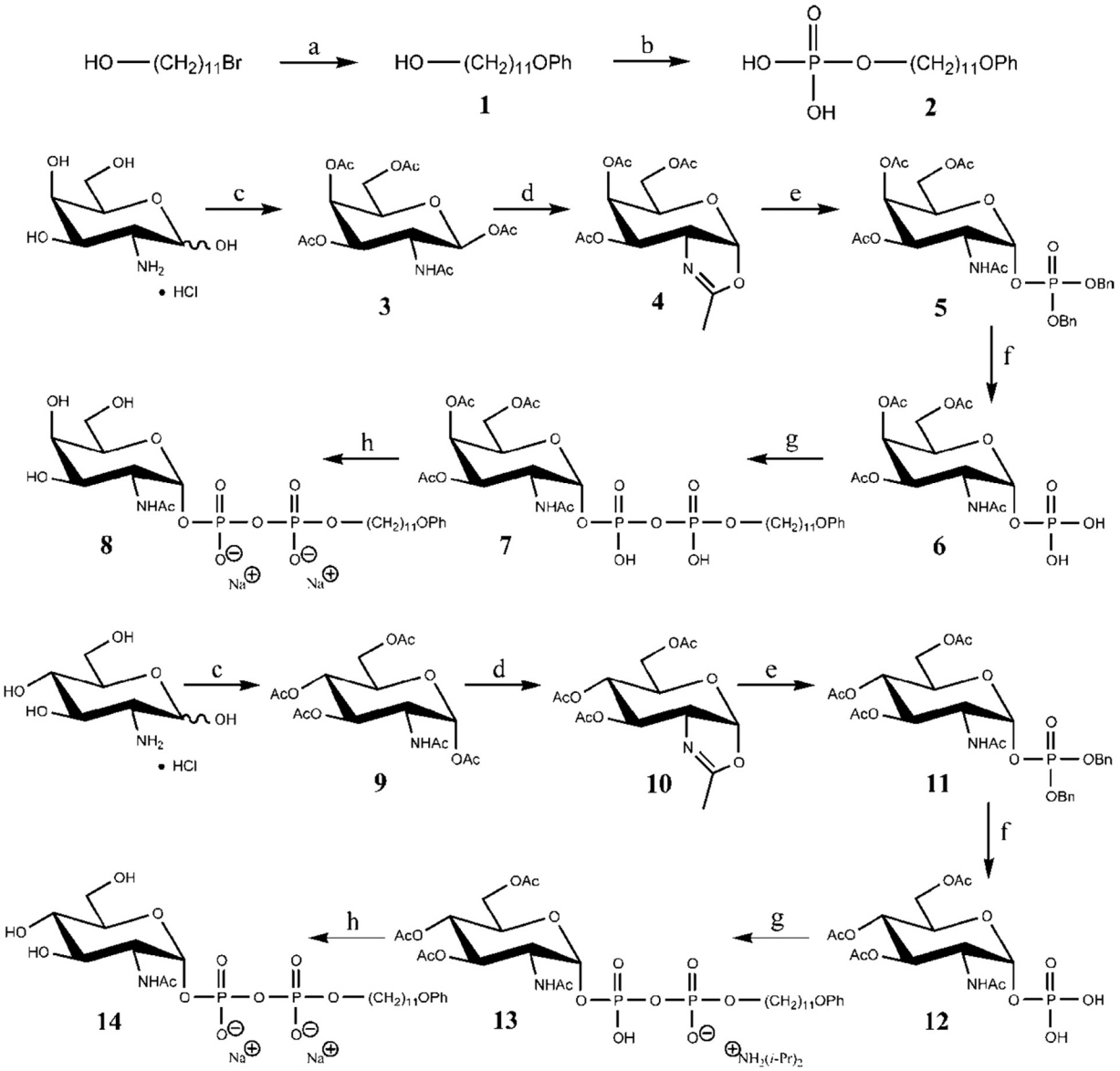

FIG 1 Synthesis of acceptor substrates 8 and 14. Reagents and conditions were as follows: PhOH, K_2CO_3, KI, acetone, reflux temperature (a); $POCl_3$, Et_3N, hexanes, 0°C → rt (b); Ac_2O, pyridine, rt (c); $CF_3SO_3Si(CH_3)_3$, 1,2-dichloroethane, 50 to 60°C (d); dibenzyl phosphate, 1,2-dichloroethane, rt (e); H_2, Pd/C, MeOH, rt (f); compound 2, diisopropylamine, 1,1′-carbonyldiimidazole, THF, rt (g); NaOMe, MeOH, rt, Amberlite IRA-120 resin (Na^+ form) (h).

nucleotide sugars to the PP-Und-linked acceptor substrates to complete the synthesis of the repeating unit. The lipid-linked saccharide is flipped across the inner membrane, and repeating units are polymerized in the periplasmic space. The completed O antigen is then ligated to the lipid A-core moiety to synthesize LPS, which is transported to the outer membrane by the Lpt complex (20, 21).

Most of the bacterial GTs are still putative and require biochemical proof of activity. We have characterized several Gal and Glc transferases that catalyze the second step in O antigen repeating-unit synthesis (22–25). The synthesis of a natural substrate analog, GlcNAcα-diphosphate phenylundecyl [GlcNAcα-O-PO_3-PO_3-$(CH_2)_{11}$-O-Ph, GlcNAc-PP-PhU], numbered 14 in Fig. 1, was instrumental in these studies (26). We recently reported that the enzyme encoded by *orf11* from *E. coli* O5 was a Gal-transferase that utilized GalNAcα-diphosphate phenylundecyl (GalNAc-PP-PhU [compound 8 in Fig. 1]) as the acceptor, as well as the fluorescent acceptor GalNAcα-diphosphate (anthracen-9-ylmethoxy)undecyl, allowing both radioactive and fluorescence-based activity assays (27). However, the enzyme had not been fully characterized. In this work, we report the thorough characterization of two WbwC Gal-transferases, the second enzymes in the assembly of repeating units from *E. coli* O104 and O5. We improved the syntheses of GalNAc-PP-PhU and GlcNAc-PP-PhU to achieve higher yields and showed that WbwC enzymes synthesize the mammalian core 1/TF antigen and can be inhibited by imidazolium salts of specific structures. The enzymes are targets for the development of antibacterial compounds and are useful for the chemoenzymatic synthesis of glycan-based vaccines that may help to prevent tumor growth.

MATERIALS AND METHODS

Materials. Reagents and materials were obtained from Sigma-Aldrich unless otherwise stated. GalNAc and GlcNAc derivatives were synthesized as described below, in the supplemental material, and in previous publications (26, 28–30). The synthesis of the undecyl (U)-containing fluorescent substrate P^1-[11-(anthracen-9-ylmethoxy)undecyl]-P^2-(2-acetamido-2-deoxy-α-D-galactopyranosyl) diphosphate (GalNAc-PP-AnthrU) was reported previously (27, 30). Glycopeptides and 4-deoxy-GalNAcα-Bn were synthesized by Hans Paulsen, University Hamburg, Hamburg, Germany. GalNAcβ1-4GlcNAcβ-Bn was synthesized by Khushi Matta at the Roswell Park Cancer Institute, Buffalo, NY. Inhibitors were synthesized as described previously (28, 30, 31).

Chemical synthesis. The syntheses of acceptor substrates 8 and 14 are shown in Fig. 1. The ether-alcohol (compound 1) was synthesized from 11-bromoundecanol by treatment with phenol-potassium carbonate-potassium iodide in acetone, following a similar procedure by Visscher et al. (32). The phosphate (compound 2) was synthesized by the treatment of alcohol 1 with phosphorus oxychloride in triethylamine-hexanes, by a modification of the procedure by Bernardes et al. (33) for the formation of citronellylphosphate. The acetylated compound 3 was synthesized by the treatment of D-galactosamine hydrochloride with acetic anhydride in pyridine. Treatment of compound 3 with trimethylsilyl triflate in 1,2-dichloroethane gave the oxazoline (compound 4), following a procedure similar to that published by Nakabayashi et al. (34). The dibenzyl phosphate (compound 5) was prepared by the treatment of oxazoline (compound 4) with dibenzyl phosphate in 1,2-dichloroethane, following essentially the procedure of Bernardes et al. (33). Hydrogenolysis of compound 5 in methanol (MeOH) using Pd/C as a catalyst gave the debenzylated sugar-phosphate (compound 6), following essentially the procedure of Montoya-Peleaz et al. (26). The coupling of the *in situ*-generated diisopropylammonium salt of phosphate 2 and sugar-phosphate 6 using 1,1′-carbonyldiimidazole in tetrahydrofuran to form compound 7, followed by deprotection of compound 7 using sodium methoxide in MeOH, gave the final acceptor substrate 8; the procedure followed was essentially that of Montoya et al. (26), but using the D-galactosamine derivative instead of the D-glucosamine derivative. The purification procedure was altered, and the enzyme-substrate reaction product was isolated and characterized in the disodium salt form. A similar synthetic strategy starting from D-glucosamine hydrochloride was followed to produce the GlcNAc-containing acceptor substrate 14, also isolated and characterized in the disodium salt form. All procedures and purification methods were modified appropriately from the existing referenced procedures. Further characterizing data, and nuclear magnetic resonance (NMR) spectroscopic data obtained in alternative solvent systems, have been obtained. These data and detailed synthetic procedures are documented in the supplemental material.

Bacterial growth, plasmids, and protein expression. The putative glycosyltransferase genes *wbwC* from *E. coli* O104 (strain G1629) and *orf11* from *E. coli* O5 (strain G1675) (see Fig. S2 in the supplemental material) were amplified by PCR, using primer pairs wl-49644/wl-49645 (5-CGGGATCCATGAAATTTAGCGTTCTGTT-3/5-CCGCTCGAGTTATTTCCGCAATATATT-3) and wl-11103/wl-11104 (5-CGGGATCCATGAATGATAGTTCAAGATCAT-3/5-CCGCTCGAGTTAATTCTTAGTCCTTGAAATAC-3), respectively. A total of 30 cycles were performed under the following conditions: denaturation at 95°C for 30 s, annealing at 50°C for 30 s, and extension at 72°C for 1 min, in a final volume of 50 μl. The amplified genes were then cloned into expression plasmid vector pET28a (KanR), containing a cleavable His tag-encoded sequence at the C terminus, and the presence of the inserts was confirmed by sequencing using an ABI 3730 sequencer. Plasmid constructs were transformed into *E. coli* BL21 for protein expression (26). For the induction of plasmid-derived enzyme, bacteria were grown overnight at 37°C in 5 ml of Luria broth containing 50 μg/ml of kanamycin with constant shaking at 150 rpm. The bacterial suspension (5 ml) was transferred to 125 ml of Luria broth containing kanamycin, and the mixture was incubated at 37°C. Isopropyl 1-thio-β-D-galactopyranoside (IPTG) was added to a final concentration of 1 mM when the suspension reached an optical density at 600 nm of 0.8. Cells were grown for an additional 4 h at 37°C and were then harvested by centrifugation for 15 min at 2,200 × *g*. Pellets were washed in phosphate-buffered saline (PBS). A total of 10 ml of PBS containing 10% glycerol was added, and aliquots of bacteria were stored at −20°C for enzyme assays.

Enzyme purification. $WbwC_{ECO104}$ and $WbwC_{ECO5}$ proteins contained a His_6 tag at the C terminus. After IPTG induction, bacteria were harvested by centrifugation, washed with PBS (pH 7.4), resuspended into the same buffer, and sonicated in four cycles for 30 s with 2-min intervals on ice (30). The homogenate was then centrifuged at 8,000 × *g* in a Centronics M-1200 centrifuge (Boehringer-Mannheim) for 30 min. The WbwC fusion proteins in the supernatant were purified using a HisPur Ni^{2+}-nitrilotriacetic acid (-NTA) Sepharose column (Thermo). Bound proteins were eluted with a gradient of 200 to 400 mM imidazole buffer in PBS. Each fraction was analyzed by sodium dodecyl-polyacrylamide gel electrophoresis (SDS-PAGE) (12% gel). The desired fractions that contained fusion protein were pooled and stored at −80°C. Western blot analysis was performed with rabbit antibody against the His_6 tag as the primary antibody (Thermo) and horseradish peroxidase-conjugated goat anti-rabbit IgG as the secondary antibody (Santa Cruz Biotechnology). Purified enzymes and cell lysates of the wild type or mutants (0.5 to 0.7 μg protein/μl) were diluted 3:1 in 4× SDS loading buffer consisting of 40 mM Tris-HCl (pH 8.0), 4% SDS, 8% glycerol, 4% β-mercaptoethanol, and bromophenol blue and run on SDS-PAGE gels (12% gel). Proteins were electrophoretically transferred onto nitrocellulose and then probed sequentially with rabbit anti-His tag antibody (1:1,000) and anti-rabbit IgG (1:10,000). Alternatively, mouse anti-His antibody and goat anti-mouse antibody (1:5,000) (Cell Biolabs Inc.) were used. Labeling was visualized with WEST-one spray (iNtRON) or Western lighting ECL Pro (Perkin-Elmer) and exposure of fluorescence on film. Prestained protein standards (GeneDirex) were used to calibrate the gels. The relative protein amounts were determined by densitometric analysis of the Western blot film, performed by using ImageJ1.43 software. The enzyme activities of purified protein were normalized according to the relative amounts of protein detected on Western blots. Protein contents were determined by measuring absorbance at 280 nm in a microvolume spectrophotometer (Nanodrop 2000; Thermo). Purified enzyme (see Fig. S3 and S4 in the supplemental material) was used for enzyme characterization.

Galactosyltransferase assays. For Gal-transferase assays, bacterial homogenates were prepared by sonication as described before (23), or purified enzyme was used as indicated. The standard assay mixtures contained, in a total of 40 μl, 0.1 mM acceptor substrate GalNAc-PP-PhU (compound 8 in Fig. 1), 5 mM $MnCl_2$, 2.5 mM dithiothreitol (DTT), 0.125 M 2-(*N*-morpholino) ethanesulfonic acid (MES) buffer, pH 7, 10 μl purified enzyme homogenate (5 to 6 μg protein), and 0.44 mM UDP-[^{3}H]Gal (2,000 to 3,500 cpm/nmol). Control assays lacked the acceptor. All assays were carried out in at least duplicate determinations, and results were confirmed by repeating the experiments at least once. Mixtures were incubated for 10 min at 37°C, and reactions were quenched by the addition of 700 μl of ice-cold water and freezing. Enzyme reaction product was isolated using Sep-Pak C_{18} columns, eluted first in water and then in MeOH, and quantified by scintillation counting as described previously (22, 25). High-pressure liquid chromatography (HPLC) separations were carried out as described previously (24), using a C_{18} column and acetonitrile-water as the mobile phase. Peaks were monitored by measuring absorbance at 195 nm and scintillation counting of fractions. Kinetic parameters were determined using the program GraphPad Prism. In assays using potential hydrophobic inhibitors, mixtures contained 10% MeOH or ethyl alcohol (EtOH) in the assay.

Enzyme reaction product identification by HPLC and MS. The enzyme reaction products were prepared in large-scale radioactive and nonradioactive forms. The separation of substrates and enzyme reaction products was achieved by HPLC using a C_{18} column at a flow rate of 1

ml/min and acetonitrile-water mixtures (27/73) as the mobile phase, monitored by absorbance at 195 nm. Product peaks were dried and analyzed by matrix-assisted laser desorption ionization–time of flight (MALDI-TOF) mass spectrometry (MS) or electrospray ionization (ESI)-MS in the negative-ion mode, as described previously (30).

Identification of enzyme reaction product structure by NMR. To prepare large amounts of nonradioactive enzyme reaction product for nuclear magnetic resonance (NMR), WbwC assays were carried out as follows. The assay mixture (20 ml) contained 4 μmol GalNAc-PP-PhU (compound 8), 30 μmol UDP-Gal, 5 ml bacterial cell homogenate in 50 mM sucrose, 0.1 mmol $MnCl_2$, and 2.5 mmol MES buffer, pH 7.0. After incubation for 60 min at 37°C, 10 ml of cold water was added to stop the reaction. The reaction mixture was then applied in aliquots to 50 C_{18} Sep-Pak columns, and the reaction products were eluted with MeOH. Following flash evaporation and lyophilization of the eluates, the reaction product was resuspended in water and further purified by reversed-phase HPLC (24) using standard compounds. Pooled fractions containing product were flash evaporated and lyophilized. Dried product was dissolved in D_2O and analyzed by 600-MHz NMR. Spectra were collected in one-dimensional (1D) and 2D experiments using a Bruker spectrometer as described previously (22).

Linkage confirmation using galactosidases or O-glycanase. The anomeric configuration of the linkage formed in the radioactive WbwC reaction product was confirmed by incubation with specific galactosidases: green coffee bean α-galactosidase (100 U/ml), *E. coli* (β1-4-specific) β-galactosidase (100 U/ml), bovine testicular (β1-3-, -4-, and -6-specific) β-galactosidase (100 U/ml), or O-glycanase (Glyko, 1.25 U/ml). Aliquots of radioactive reaction product (2,000 cpm) were treated in a total volume of 100 μl with 25 μl MacIlvaine buffer (0.1 M citric acid–0.2 M Na-phosphate, pH 4.3), 10 μl 0.1% bovine serum albumin, and galactosidase or O-glycanase. The activities of galactosidases were confirmed with Galα- and Galβ-*p*-nitrophenyl as the substrates. Control incubations lacked the enzymes. Mixtures were incubated for 30 min at 37°C, diluted with 800 μl of water, and applied to columns of 0.4 ml AG1x8 (Cl^- form). Released radioactivity was eluted with 2.8 ml water and quantified, while unreacted negatively charged WbwC reaction products stayed bound to the AG1x8 columns.

Test for TF antigen cross-reactivity. To test whether the enzyme reaction products represented the cancer-associated TF antigen, JAAFII mouse monoclonal antibody against the TF antigen was used as the primary antibody (kindly donated by K. Rittenhouse, Roswell Park Cancer Institute, Buffalo, NY, USA) and horseradish peroxidase-conjugated goat anti-mouse IgG as the secondary antibody (Santa Cruz Biotechnology). A 50-nmol amount of either $WbwC_{ECO104}$ or $WbwC_{ECO5}$ reaction product Galβ1-3GalNAcα-PP-PhU, WbdN reaction product Glcβ1-3GlcNAcα-PP-PhU (23), compound 8 or its GlcNAc derivative 14, or Galβ1-3GalNAcα-Bn as the positive TF antigen control was incubated with 0.5 ml 1:100 TF antigen-specific antibody (4 mg/ml in Tris-buffered saline) overnight at 4°C. This was followed by incubation with 200 ng secondary antibody (goat anti-mouse IgG, 1:1,000) for 2 h at room temperature (rt). A 2-μl volume was saved as a positive control for antibody, and the remainder was slowly loaded onto C_{18} Sep-Pak columns. Columns were washed first with 5 ml water and then with 5 ml MeOH. MeOH fractions were dried by rotary evaporation and dissolved in 500 μl H_2O. Samples were then transferred to small tubes, lyophilized, and dissolved in 10 μl H_2O. Samples were spotted onto nitrocellulose membrane and dried. Labeling was visualized with WEST-one spray (iNtRON) and exposure of fluorescence on film.

Effect of amino acid-specific reagents. To evaluate the role of amino acids in Gal-transferase activity, the purified enzyme preparations were incubated with amino acid-specific reagents prior to the assays for 10 min at rt in reaction mixtures lacking UDP-Gal. The reaction was initiated by the addition of UDP-Gal. *p*-Hydroxyphenylglyoxal (HPG; reacts with Arg), 5,5′-dithio-bis-2-nitrobenzoic acid (DTNB; reacts with Cys), and *N*-ethylmaleimide (NEM; reacts with Cys) were used at 0.2 mM concentration in the assay. Disulfide bond-reducing agent dithiothreitol was used at 0.1 to 4 mM in the assay and β-mercaptoethanol (beta-ME) at 1 to 18 mM.

Construction of $WbwC_{ECO104}$ mutants. The QuikChange site-directed mutagenesis kit (Agilent, Santa Clara, CA) was used to construct mutants D91A and D125A of $Wbw_{CECO104}$. Primers were designed using the Quikchange Primer Design program. For the D91A mutant, the forward primer was 5′CAATGAACTGATTTTTAGGATGGCTACTGATGATATTT GTTTGCCTG3′ and the reverse primer was 5′CAGGCAAACAAATATCAT CAGTAGCCATCC AAAAATCAGTTCATTG3′. For the D125A mutant, the forward primer was 5′GGGAAGTGTCATTGAAGAATTTGCTAATACAA TGAAAATTAGGCAAG3′ and the reverse primer was 5′CTTGCCTAATTT TCATTGTATTAGCAAATTCTTCAATGGCACTTCCC3′. Amplification was performed with a DNA thermal cycler (model Eppendorf Mastercycler Gradient) by using a single denaturation step at 95°C for 1 min followed by an 18-cycle program consisting of denaturation at 95°C for 1 min, annealing at 55°C for 1.5 min, and extension at 68°C for 6 min. A total of 10 μl of each reaction mixture was electrophoresed on a 1% agarose gel in 45 mM Tris-borate buffer–1 mM EDTA, pH 8.3, at 150 V for 1 h and stained with ethidium bromide. The PCR mixture was transformed into *E. coli* Top10 cells. Bacterial colonies harboring mutated genes were isolated, and plasmids were isolated and sequenced (Robarts Research Institute, London, ON, Canada) to confirm the correct mutations. Mutants D45A, D46A, D93A, D94A, C21A, C82A, and C96A of $Wbw_{CECO104}$ and mutants D96A, D98A, and D99A of Wbw_{CECO5} were constructed by Mutagenex (Hillsborough, NJ). Bacterial growth, enzyme activity assays, SDS-PAGE, and Western blotting were carried out as described above.

RESULTS

Sequence comparisons of $WbwC_{ECO104}$ and $WbwC_{ECO5}$. A protein-protein BLAST comparison revealed that the amino acid sequences of $WbwC_{ECO104}$ and $WbwC_{ECO5}$ have 47% identity (see Fig. S2 in the supplemental material). WbwC from *E. coli* O104 shares 42% identity with uncharacterized WbwC from *E. coli* O81, 99% identity with WbwC from *Escherichia fergusonii* (35), and 79% identity with WfaM from *E. coli* O24 (36). Homologs of WbwC are also found in a number of other bacterial strains. None of these enzymes have been characterized. The other putative glycosyltransferases (WbwA and WbwB) encoded by genes located in the O104 antigen gene cluster (18) share only 13% and 11% identity, respectively, with $WbwC_{ECO104}$. WbiP from *E. coli* O127 (37), which also synthesizes a Galβ1-3GalNAc linkage, shows only 22% and 25% sequence identity with $WbwC_{ECO104}$ and $WbwC_{ECO5}$ (see Fig. S2 in the supplemental material). WbbD from *E. coli* O7 (26) and WbgO from *E. coli* O55 (38) both form a Galβ1-3GlcNAc linkage. WbbD shares 37% and 35% sequence identity with $WbwC_{ECO104}$ and $WbwC_{ECO5}$, respectively, whereas WbgO shares 23% and 20% sequence identity with $WbwC_{ECO104}$ and $WbwC_{ECO5}$. Human core 1 Gal-transferase (C1GalT1), which also forms a Galβ1-3GalNAc linkage, shows very low sequence identity to $WbwC_{ECO104}$ (12%) and to $WbwC_{ECO5}$ (11%). WbwC is predicted to form a GT-A glycosyltransferase fold and has been classified in the CAZy GT2 family, which includes many other bacterial and mammalian inverting β-glycosyltransferases (22–24, 37–39). All of the WbwC homologs have a DxD sequence that might be involved in catalysis (40).

Properties of $WbwC_{ECO104}$ and $WbwC_{ECO5}$. Based on the amino acid composition, the molecular masses of His_6-tagged $WbwC_{ECO104}$ and $WbwC_{ECO5}$ were calculated to be 31.2 and 31.4 kDa, respectively (protein molecular mass calculator; Science Gateway, www.sciencegateway.org). The two recombinant proteins from the bacterial lysate were induced by 1 mM IPTG in a 4-h

incubation at 37°C and showed intense bands on SDS-PAGE at an apparent molecular mass of 30 to 32 kDa. Induction at rt, overnight or after 6 h at 0.5 or 1 mM IPTG did not improve the level of expression. The His_6-tagged $WbwC_{ECO104}$ and $WbwC_{ECO5}$ were purified by NTA Sepharose affinity chromatography (see Fig. S3 and S4 in the supplemental material). Western blotting showed a major protein band at 30 kDa for $WbwC_{ECO104}$ for both the cell lysate and the purified enzyme at about 90% purity. $WbwC_{ECO5}$ was expressed and purified similarly but was slightly larger (32 kDa). A single elution with 150 mM imidazole was optimal for eluting the protein from the NTA column (about 50% purity). The specific activities of purified $WbwC_{ECO104}$ and $WbwC_{ECO5}$ were enriched 49-fold and 14-fold, respectively. The final yield of purified $WbwC_{ECO104}$ and $WbwC_{ECO5}$ proteins obtained from 150 ml starting culture was 5 to 7 mg (0.6 mg/ml). Under standard conditions, the transfer of Gal to GalNAcα-O-PO_3-PO_3-$(CH_2)_{11}$-O-Ph was linear for up to 10 min of incubation time and up to 6 μg protein per assay for purified $WbwC_{ECO104}$ and $WbwC_{ECO5}$. Gal-transferase activities in the bacterial homogenates were stable for several days at rt for at least 2 weeks at 4°C and for at least 4 months at −20°C.

The presence of the conserved DxD motif (DTDD in the $WbwC_{ECO104}$ and DSDD in the $WbwC_{ECO5}$ sequence) suggested the involvement of divalent metal cations as cofactors in Gal-transferase catalysis (40, 41). No activity was observed in the presence of 5 mM EDTA. At 5 mM concentration, Mn^{2+} was the most efficient cofactor among the divalent metal ions (set to 100% activity), but Mg^{2+} also stimulated the activity (22% for $WbwC_{ECO104}$ and 15% for $WbwC_{ECO5}$). The optimal concentration of Mn^{2+} in the WbwC assays was between 2.5 and 5 mM (data not shown). None of the other metal ions tested at 5 mM concentration (Co^{2+}, Pb^{2+}, Ca^{2+}, Zn^{2+}, and Cu^{2+}) were effective in stimulating WbwC Gal-transferase activity. Both $WbwC_{ECO104}$ and $WbwC_{ECO5}$ activities were shown to have a broad pH optimum between 7 and 8 (data not shown).

Effects of detergents on $WbwC_{ECO104}$ and $WbwC_{ECO5}$ activity. The hydrophobicity plots of both WbwC enzymes did not reveal any transmembrane domains, but *in vivo*, the enzymes could be loosely associated with the bacterial membrane. Membrane components or detergents could also affect the availability of the sugar-diphosphate-lipid acceptor substrate. We therefore determined whether the purified $WbwC_{ECO104}$ enzyme activity was affected by the presence of 0.125 to 0.5% Triton X-100, NP-40 (nonyl phenoxylpolyethoxylethanol), or n-octyl-β-D-glucoside (Octylglucoside). There was no effect with NP-40 treatment, but the presence of the other detergents reduced $WbwC_{ECO104}$ Gal-transferase activities to various degrees (data not shown). Interestingly, the effect of detergents on $WbwC_{ECO5}$ enzyme activity differed from the effect on $WbwC_{ECO104}$, and $WbwC_{ECO5}$ activity was reduced by all detergents tested. SDS at 0.005% in the reaction mixtures completely abolished both $WbwC_{ECO104}$ and $WbwC_{ECO5}$ activities.

Acceptor substrate specificities of $WbwC_{ECO104}$ and $WbwC_{ECO5}$. The acceptor substrate specificities of purified $WbwC_{ECO104}$ and $WbwC_{ECO5}$ were tested with a series of synthetic acceptor substrate analogs, including compounds 8 and 14, GalNAcα-glycopeptides, GalNAc α and β linked to a number of different hydrophobic aglycone groups, and GlcNAc derivatives (Table 1). The only two compounds in this series that could serve as acceptor substrates were GalNAc-PP-PhU (compound 8) and a fluorescent acceptor (GalNAc-PP-AnthrU), but the corresponding GlcNAc analog GlcNAc-PP-PhU or any other GalNAc or GlcNAc derivative could not. This suggested that the presence of a diphosphate bridge in the acceptor as well as the axial 4-hydroxyl of the acceptor sugar was required for the activity of both $WbwC_{ECO104}$ and $WbwC_{ECO5}$. The kinetic parameters for purified $WbwC_{ECO104}$ and $WbwC_{ECO5}$ were similar, with apparent K_m values of 0.12 mM and 0.10 mM, respectively, for GalNAc-PP-PhU, and apparent maximum rate of metabolism (V_{max}) values of 1.57 μmol/h/mg for $WbwC_{ECO104}$ and 1.42 μmol/h/mg for $WbwC_{ECO5}$ (Fig. 2). For UDP-Gal, the apparent K_m values for $WbwC_{ECO104}$ and $WbwC_{ECO5}$ were 0.73 mM and 1.20 mM, respectively, with apparent V_{max} values of 0.87 μmol/h/mg and 2.67 μmol/h/mg, respectively. At high acceptor concentration, substrate inhibition was observed. These values were similar to those obtained with crude enzymes.

TABLE 1 Acceptor substrate specificities of $WbwC_{ECO104}$ and $WbwC_{ECO5}$[a]

Compound	Concn(mM)	Relative activity	
		$WbwC_{ECO104}$	$WbwC_{ECO5}$
GalNAcα-PO_3-PO_3-$(CH_2)_{11}$-O-Ph (compound 8)	0.1	100	100
GalNAcα-PO_3-PO_3-AnthrU[b]	0.1	49.0	46.1
GlcNAcα-PO_3-PO_3-$(CH_2)_{11}$-O-Ph (compound 14)	1	<1	<1
GalNAcα-Bn	1	<1	<1
4-Deoxy-GalNAcα-Bn	1	<1	<1
A-(GalNAcα)T	1	<1	<1
N-Ac-V-(GalNAcα)TP-NH_2	1	<1	<1
GalNAc	1	<1	<1
AHGVT-(GalNAcα)SAPDTRPAPGSTAPPA	1	<1	<1
GalNAcβ1–4GlcNAcβ-Bn	1	<1	<1

[a] Neutral compounds were assayed by the AG1 × 8 method; compounds 8 and 14 and GalNAcα-PO_3-PO_3-AnthrU were assayed by the C_{18} Sep-Pak method with 0.435 mM UDP-Gal in the assay (23, 28, 29).
[b] The compound solution contained other minor components.

Donor specificities of $WbwC_{ECO104}$ and $WbwC_{ECO5}$. The donor specificities of purified $WbwC_{ECO104}$ and $WbwC_{ECO5}$ were examined by replacing 0.435 mM UDP-[^{3}H]Gal with a number of other nucleotide sugars in the assay at the same concentration. No activities were observed with UDP-[^{3}H]Glc, UDP-[^{3}H]GalNAc, UDP-[^{3}H]GlcNAc, CMP-[^{3}H]sialic acid, or GDP-[^{3}H]Man. This was indicative of a strict specificity of $WbwC_{ECO104}$ and $WbwC_{ECO5}$ for UDP-Gal as the donor substrate.

Analysis of $WbwC_{ECO104}$ and $WbwC_{ECO5}$ reaction products. To determine the structures of $WbwC_{ECO104}$ and $WbwC_{ECO5}$ reaction products, aliquots of assay mixtures were applied to Sep-Pak C_{18} columns and enzyme reaction product was eluted with MeOH. MALDI-MS analysis of the MeOH eluates showed the presence of substrate (*m/z* 626) and enzyme product (*m/z* 788) (data not shown). The Sep-Pak step was required for the efficient HPLC separation of the reaction product. On reversed-phase HPLC, using 24% acetonitrile–76% water as the mobile phase, the product Gal-GalNAc-PP-PhU eluted between 35 and 45 min, well separated from substrate. The radioactive product served as a standard for HPLC. Pooled fractions containing purified reaction products showed *m/z* 788 for Gal-GalNAc-PP-PhU by MALDI-MS. This demonstrated that one Gal residue (*m/z* 162) had been added to the substrate by both $WbwC_{ECO104}$ and $WbwC_{ECO5}$.

NMR analysis of WbwC reaction products. The ^{1}H-NMR spectrum of the $WbwC_{ECO104}$ product showed a new doublet at

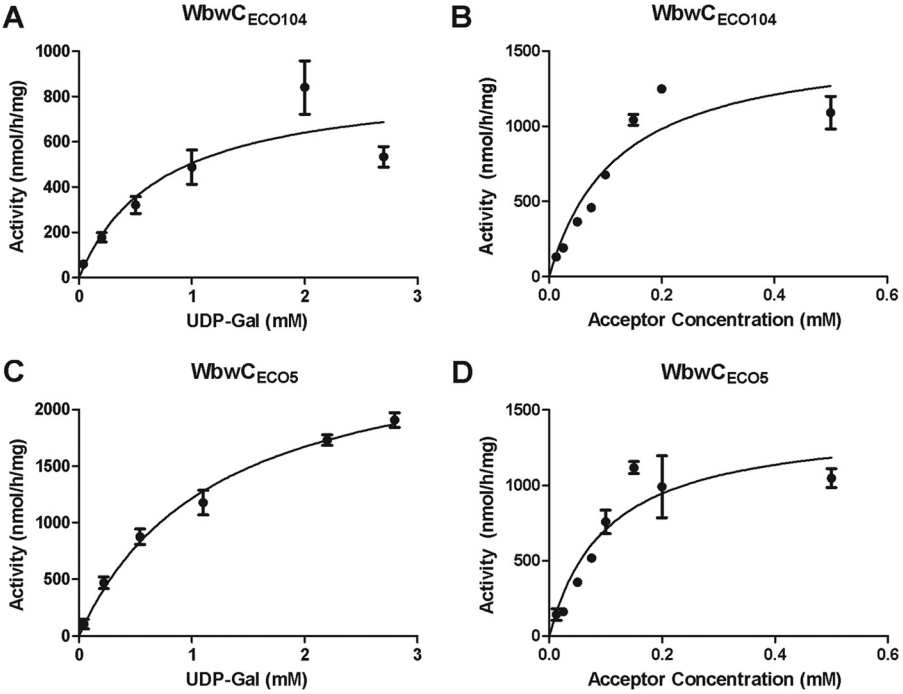

FIG 2 Kinetics of WbwC$_{ECO104}$ and WbwC$_{ECO5}$ reactions. The standard assay as described in Materials and Methods was used to measure Gal transfer by purified WbwC enzymes. (A) WbwC$_{ECO104}$ reaction with acceptor 8 (0.25 mM) as a function of UDP-Gal concentration. The apparent K_m for UDP-Gal was 0.73 mM with an apparent V_{max} of 0.87 μmol/h/mg protein. (B) WbwC$_{ECO104}$ reaction as a function of acceptor 8 concentration. UDP-Gal concentration was 2.2 mM. The apparent K_m for 8 was 0.12 mM with an apparent V_{max} of 1.57 μmol/h/mg protein. (C) WbwC$_{ECO5}$ reaction with 0.25 mM acceptor 8 as a function of UDP-Gal concentration. The apparent K_m for UDP-Gal was 1.20 mM with an apparent V_{max} of 2.67 μmol/h/mg protein. (D) WbwC$_{ECO5}$ reaction as a function of acceptor 8. UDP-Gal donor concentration was 1.09 mM. The apparent K_m for acceptor 8 was 0.10 mM with an apparent V_{max} of 1.42 μmol/h/mg protein. Substrate inhibition was apparent at high acceptor concentration (not shown). All results were analyzed by regression analysis with GraphPad Prism.

TABLE 2 ^{1}H and ^{13}C NMR parameters of WbwC$_{ECO104}$ enzyme substrate 8 and WbwC$_{ECO104}$ reaction product Galβ1-3GalNAcα-PO$_3$-PO$_3$-(CH$_2$)$_{11}$-O-Ph[a]

Residue	^{1}H (ppm)	^{13}C (ppm)
WbwC reaction product Galβ1-3GalNAcα-PO$_3$-PO$_3$-(CH$_2$)$_{11}$-O-Ph		
Gal-1	4.41 $J_{1,2}$ = 8.3 Hz	104.5
Gal-2	3.45	70.7
Gal-3	3.55	72.1
Gal-4	3.82	68.3
Gal-5	3.57	74.5
Gal-6	3.65	60.2
GalNAc-1	5.45 $J_{1,2}$ = 7.2 Hz, 3.7 Hz	94.7
GalNAc-2	4.32	48.2
GalNAc-3	4.00	77.1
GalNAc-4	4.19	68.4
GalNAc-5	4.13	71.6
GalNAc-6	3.67	60.6
GalNAc-N-acetyl	1.97	
Substrate 8, GalNAcα-PO$_3$-PO$_3$-(CH$_2$)$_{11}$-O-Ph		
GalNAc-1	5.39 $J_{1,2}$ = 7.0 Hz, 3.4 Hz	94.6
GalNAc-2	4.13	49.8
GalNAc-3	3.78–3.88	66.9
GalNAc-4	3.90–3.94	67.3
GalNAc-5	4.07	72.1
GalNAc-6	3.58, 3.69	61.1
GalNAc-N-acetyl	2.00	

[a] The substrate for the WbwC$_{ECO104}$ reaction was GalNAcα-PO$_3$-PO$_3$-(CH$_2$)$_{11}$-O-Ph (compound 8 in Fig. 1) as described in Materials and Methods. Enzyme reaction product was purified by Sep-Pak C18 column and reversed-phase HPLC; 600-MHz NMR spectra were collected in 1D and 2D experiments in D_2O. Assignments were made by HSQC and ROESY spectra. The coupling constants were difficult to determine with certainty due to crowding of signals. The spectra for the WbwC$_{ECO5}$ reaction product were virtually identical to those shown for the WbwC$_{ECO104}$ reaction product.

4.41 ppm for H-1 of Gal with a coupling constant of $J_{1,2}$ = 8.3 Hz, which is indicative of Gal in β-linkage (Table 2 and Fig. 3). By comparison, the spectrum of the enzyme reaction product of β3-GalT WbbD (Galβ1-3GlcNAc-PP-PhU) showed a similar chemical shift for Gal H-1 at 4.35 ppm (24). To determine whether Gal was β1-3, β1-4, or β1-6 linked to GalNAc, we conducted two-dimensional NMR experiments, including rotating-frame nuclear Overhauser effect correlation spectroscopy (ROESY) (Fig. 4) and heteronuclear single quantum coherence (HSQC), which identified the carbon and proton chemical shifts of the Gal and GalNAc residues (Table 2). The GalNAc H-3 signal of substrate 8 (3.78 to 3.88 ppm) shifted to 4.00 in the WbwC reaction product. A large difference between substrate and product in the ^{13}C signals was also seen for the GalNAc C-3 signal, which was 66.9 ppm in the substrate and 77.1 ppm in the product. However, the GalNAc H-4 signal also shifted from 3.90 to 3.94 ppm to 4.19 ppm in the product, but neither H-6 nor C-4 or C-6 signals showed large differences between substrate and product. A strong coupling between Gal H-1 and GalNAc H-3 was seen in the ROESY spectrum (Fig. 4), showing that Gal was indeed linked to position 3 of GalNAc. The NMR spectra of WbwC$_{ECO5}$ reaction product (data not shown) were virtually identical to those from WbwC$_{ECO104}$. This identifies the product structures as Galβ1-3GalNAcα-PP-PhU and proves that WbwC is a UDP-Gal:GalNAc-diphosphate-R β1,3-Gal-transferase.

Glycosidase digestions of WbwC enzyme reaction products. Galactosidase digestions were used to confirm the anomeric linkage between Gal and GalNAc in the [^{3}H]Gal-GalNAc-

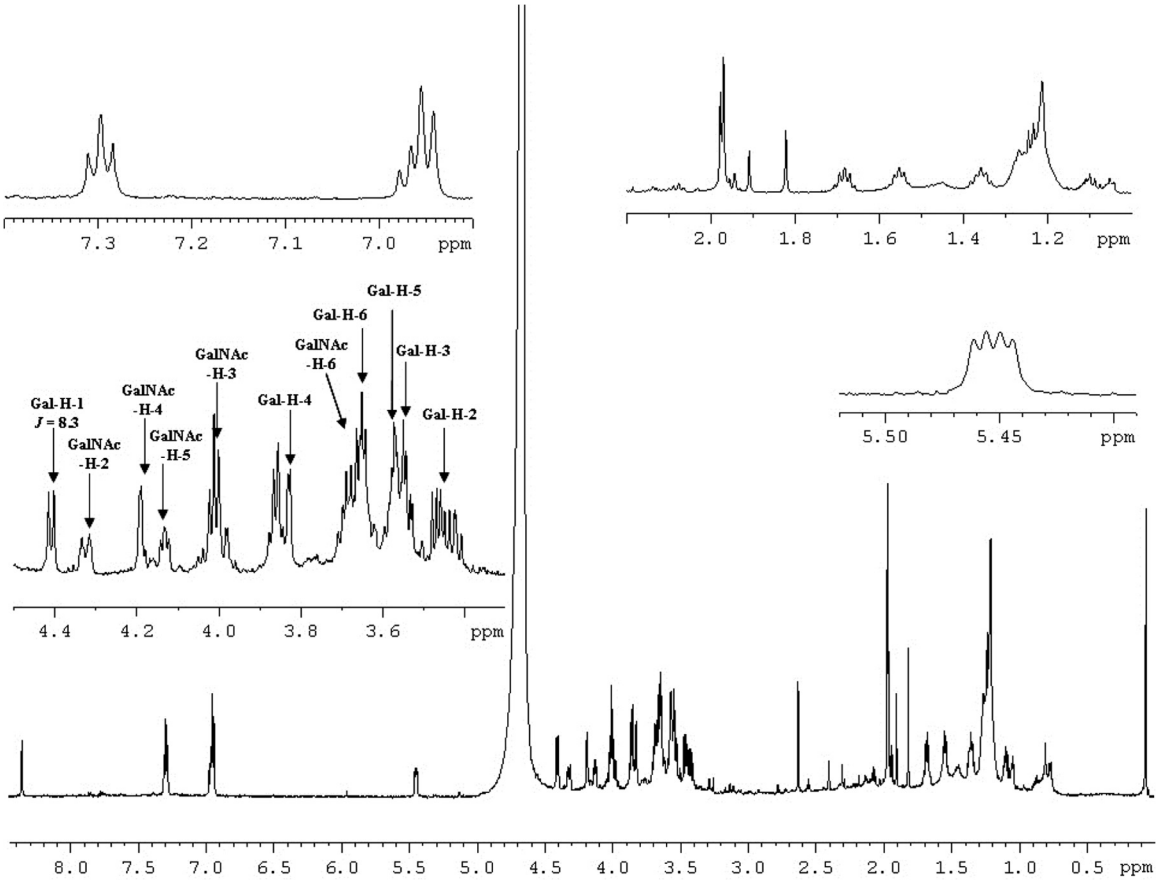

FIG 3 One-dimensional 600-MHz ^{1}H-NMR spectra of WbwC$_{ECO104}$ Gal-transferase reaction product measured in D_2O. WbwC$_{ECO104}$ and WbwC$_{ECO5}$ reaction products have virtually identical spectra. Sample preparation is described in Materials and Methods.

PP-PhU enzyme reaction products synthesized by WbwC$_{ECO104}$ and WbwC$_{ECO5}$. The released free [^{3}H]Gal was separated by AG1x8 columns that bound the uncleaved reaction product. WbwC$_{ECO104}$ and WbwC$_{ECO5}$ reaction products were resistant to green coffee bean α-galactosidase and to Jack bean (β1-4-specific) β-galactosidase, indicating that Gal was not α linked or in β1-4 linkage (Fig. 5). In contrast, treatment with bovine testicular β-galactosidase, which cleaves Gal in β1-3, β1-4, and β1-6 linkages, released 41% and 36% of the radioactivity from WbwC$_{ECO104}$ and WbwC$_{ECO5}$ reaction products, respectively. O-glycanase is an enzyme that cleaves O-glycan core 1, Galβ1-3GalNAcα, from glycopeptides and core 1-linked hydrophobic compounds, but it was not known if the enzyme also acts on diphosphate-linked core 1 structures. Indeed, O-glycanase released 29% and 32% of the radioactivity from the disaccharide reaction products of WbwC$_{ECO104}$ and WbwC$_{ECO5}$. This enzyme therefore acts on a variety of core 1-containing glycoconjugates, including those with negatively charged diphosphates attached to core 1. These results confirm that the WbwC reaction products have the structure Galβ1-3GalNAcα-PP-PhU.

Cross-reactivity of WbwC enzyme reaction products with TF antigen-specific antibody. To test whether the enzyme reaction products represented the TF antigen in spite of the presence of the diphosphate group, aliquots of reaction products (50 nmol) were incubated with TF antigen-specific antibody as the primary antibody and horseradish peroxidase-conjugated anti-mouse IgG as the secondary antibody. The complexes were then separated by C_{18} Sep-Pak, which binds the hydrophobic phenylundecyl moiety. As a positive control, core 1–benzyl was used, and the substrate GalNAc-PP-PhU, the corresponding GlcNAc-PP-PhU, and the WbdN reaction product Glcβ1-3GalNAcα-PP-PhU (23) were used as negative controls. After washing with water, MeOH elution fractions were concentrated and applied to nitrocellulose membrane and stained for peroxidase activity. The results showed that after separation by C_{18} Sep-Pak, only the positive control and WbwC$_{ECO104}$ and WbwC$_{ECO5}$ reaction products stained positively for the TF antigen (see Fig. S5 in the supplemental material). It is interesting that Gal-GalNAc-PP-PhU bound to C_{18} Sep-Pak in the presence of antibodies and that the core 1 structure was clearly recognized by the antibody as the TF antigen, in spite of being linked to a charged diphosphate-lipid group. This confirms that both WbwC$_{ECO104}$ and WbwC$_{ECO5}$ synthesized the TF antigen.

Role of specific amino acids in WbwC$_{ECO104}$ and WbwC$_{ECO5}$ activities. There are many positively charged amino acid residues in WbwC$_{ECO104}$ and WbwC$_{ECO5}$ that may possibly be involved in the binding of the negatively charged substrates, and we previously identified an essential Lys residue in Gal-transferase WfeD (25). The inclusion of 0.2 mM HPG in the assay mixture (without DTT) for purified WbwC enzymes showed 22% inhibition of WbwC$_{ECO104}$ activity and minimal inhibition of WbwC$_{ECO5}$ activity (Fig. 6). This suggested a potential role of Arg in the protein structure or catalysis of WbwC$_{ECO104}$.

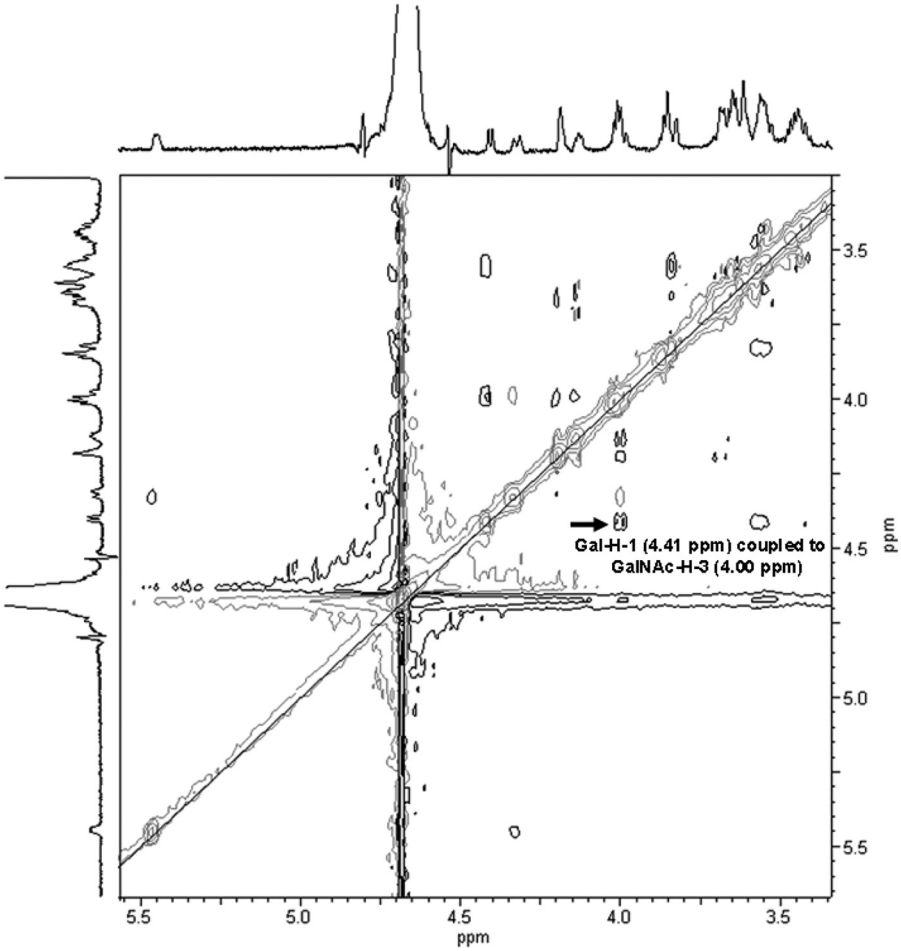

FIG 4 Two-dimensional 600-MHz ROESY spectrum of $WbwC_{ECO104}$ Gal-transferase reaction product measured in D_2O. Experiments were performed at rt. There is a clear correlation between the Gal H-1 and GalNAc H-3 signals indicating the Gal1-3GalNAc linkage.

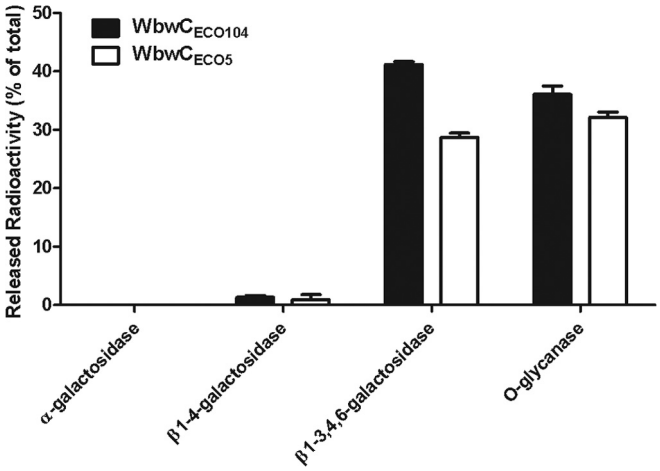

FIG 5 Glycosidase digestion of WbwC reaction products. Product linkage confirmation using glycosidase digestion on WbwC reaction products. The anomeric configuration of the linkage formed in the radioactive enzyme product was determined by incubation with specific galactosidases or O-glycanase. Mixtures were incubated for 30 min at 37°C and applied to AG1x8 columns. Released radioactivity was eluted and quantified. The percentages of release of radioactive Gal (or Gal-GalNAc for O-glycanase) are shown relative to the total radioactivity of WbwC reaction products in the assay. The bars indicate variations between duplicates.

There are a number of conserved Cys residues in $WbwC_{ECO104}$. In the absence of DTT, DTNB (0.2 mM), which reacts with reduced SH groups, inhibited $WbwC_{ECO104}$ and $WbwC_{ECO5}$ activities by 49% and 81%, respectively, while 0.2 mM NEM showed 10% and 45% inhibition, respectively. In contrast, DTT (0.2 mM), which reduces disulfide bonds, stimulated $WbwC_{ECO104}$ and $WbwC_{ECO5}$ activities. β-Mercaptoethanol (18 mM) also increased the activities of $WbwC_{ECO104}$ and $WbwC_{ECO5}$ by 30% and 75%, respectively (Fig. 6). This suggested that enzymes may have formed disulfide bonds upon storage that interfered with activity, although these cytosolic enzymes are expected to be naturally in the reduced state. All of the Cys mutants of $WbwC_{ECO104}$ (C21A, C82A, and C96A) were fully active, indicating that these Cys residues are not required for activity. Reagents that covalently bind to Cys-SH groups may thus lead to less active enzyme by blocking the access of substrates.

Importance of a novel DxDD motif for $WbwC_{ECO104}$ and $WbwC_{ECO5}$ activity. Most inverting glycosyltransferases have a DxD motif, which can contain an Asp or Glu residue representing a catalytic base (40). The WbwC sequences contain a DxDD motif that had not yet been recognized and is conserved mainly in β3-glycosyltransferases within the GT2 family. To evaluate the roles of these acidic amino acids, Asp residues were mutated to the

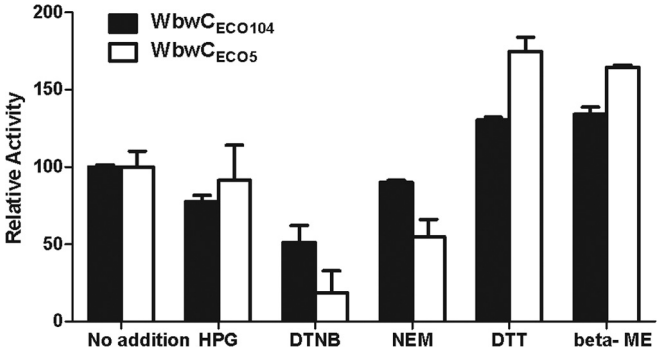

FIG 6 Effects of amino acid-specific reagents on activity of WbwC. Amino acid-specific reagents were preincubated with purified enzyme for 10 min, prior to the assays as described in Materials and Methods. The activities are shown relative to the positive control set to 100 (no addition of amino acid reagent). The bars indicate variations between duplicates. HPG, 0.2 mM hydroxyphenylglyoxal; DTNB, 0.2 mM 5,5′-dithio-bis-2-nitrobenzoic acid; NEM, 0.2 mM *N*-ethylmaleimide; DTT, 0.2 mM dithiothreitol; beta-ME, 18 mM beta-mercaptoethanol.

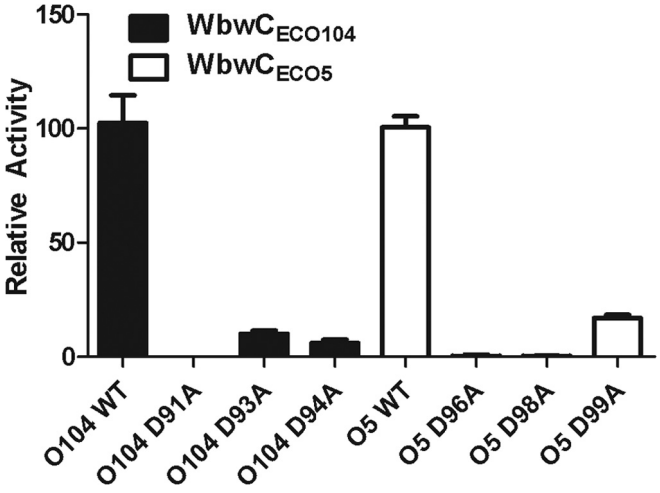

FIG 7 Relative activities of site-specific mutants of the DxDD motif of WbwC$_{ECO104}$ and WbwC$_{ECO5}$. Mutants of WbwC$_{ECO104}$ and WbwC$_{ECO5}$ were produced by replacing Asp with Ala as indicated and assayed as described in Materials and Methods. WT, wild type (unaltered controls of WbwC$_{ECO104}$ and WbwC$_{ECO5}$ set to 100). Relative activities are shown with error bars indicating differences in activities between multiple assays. Western blots showed that all mutants were well expressed.

neutral Ala in WbwC$_{ECO104}$ and WbwC$_{ECO5}$. Mutations of any of the Asp residues within the DTDD sequence in WbwC$_{ECO104}$ and the DSDD sequence in WbwC$_{ECO5}$ were found to drastically reduce the activities of both WbwC$_{ECO104}$ (residues D91, D93, and D94) and WbwC$_{ECO5}$ (residues D96, D98, and D99). No activity was detected with mutants lacking the first Asp residue of the DxDD motif (D91A mutant of WbwC$_{ECO104}$ and D96A mutant of WbwC$_{ECO5}$) (Fig. 7). In contrast, none of the other conserved Asp residues in the WbwC$_{ECO104}$ enzyme appeared to contribute to catalysis, and D45A, D46A, and D125A mutants had activities comparable to that of the wild-type enzyme. All mutants were well expressed, as shown by SDS-PAGE and Western blots (data not shown). This suggests that the WbwC enzyme family has a novel DxDD motif in which the first Asp residue is essential and the remaining Asp residues are important for catalysis.

Inhibition of WbwC$_{ECO104}$ and WbwC$_{ECO5}$ activity. A number of diimidazolium salts, i.e., those having two positively charged imidazolium groups linked by aliphatic chains of 20 to 22 carbons, strongly inhibited WbwC$_{ECO104}$ and WbwC$_{ECO5}$ activities in the absence of DTT in the assay (Table 3). The solvents alone, without inhibitors (up to 10% in the assay) showed no effect. Especially compound QT 149 [1,22-bis-(3-methyl-1H-imidazolium-1-yl)docosane dimesylate], having an aliphatic chain of 22 carbons in length, effectively inhibited purified WbwC$_{ECO104}$ and WbwC$_{ECO5}$ with 50% inhibitory concentrations (IC_{50}s) of 8.0 μM and 17.6 μM, respectively. In contrast, inhibitors of mammalian β1,4-Gal-transferase (N-butyryl-glucosamine-β-1-thio-2-naphthyl) (29) and core 1 β1,3-Gal-transferase (N-butyryl-galactosamineα-Bn) (39) showed no inhibition.

DISCUSSION

Two similar enzymes, WbwC$_{ECO104}$ and WbwC$_{ECO5}$, have been identified as UDP-Gal:GalNAcα-diphosphate-lipid β1,3-D-Gal-transferases that catalyze the second step of the O antigen repeating-unit assembly in *E. coli* serotypes O104 and O5, respectively. The enzymes have the same function in synthesizing the Galβ1-3GalNAc linkage and have very similar properties, although the amino acid sequences show only 47% identity.

Analyses of the structures of the WbwC$_{ECO104}$ and WbwC$_{ECO5}$ enzyme reaction products by HPLC, MS, and NMR spectroscopy, by digestions with galactosidases and O-glycanase, and by Western blots using TF antigen-specific antibody clearly showed that both WbwC enzymes add one Gal residue in β1-3 linkage to GalNAc-PP-PhU, an analog of the natural undecaprenyl-linked substrate. The reaction product structure corresponds to the disaccharide at the reducing end of the O104 and O5 antigen repeating unit and establishes WbwC$_{ECO104}$ and WbwC$_{ECO5}$ as the second enzymes in the respective O104 and O5 antigen repeating-unit biosynthesis pathways.

There are several bacterial strains that have the internal Galβ1-3GalNAc linkage in their O antigen structures (14, 15, 42). The β1,3-Gal-transferase WbiP has been characterized from *E. coli* O127, which contains the internal Galβ1-3GalNAcα structure in the O antigen (37). WbiP synthesizes the Galβ1-3GalNAcα linkage but does not have a requirement for the diphosphate group in the acceptor and can act on free GalNAc, with a preference for the GalNAcα linkage. Thus, a number of simple oligosaccharides serve as the WbiP substrate, and these assays do not require extensive chemical synthesis of complex sugar-phosphates. We describe improved syntheses of GalNAc-PP-PhU and GlcNAc-PP-PhU in this paper, which should enhance the characterization of other bacterial enzymes with yet-unknown function that may require the diphosphate group in the acceptor substrate.

Like other characterized members of the GT2 family, WbwC enzymes are typical inverting transferases, requiring divalent metal ion for activity and having DxD motifs (40, 41). We have shown in this study that all three Asp residues of the DxDD motif are required for full activity in both WbwC$_{ECO104}$ and WbwC$_{ECO5}$, with the first Asp being essential for activity and likely representing the catalytic base, and the other two Asp residues likely contributing to the acidic properties of the first Asp residue. Thus, we identified a new DxDD motif that is found in several members of the GT2 family. These enzymes have a predicted GT-A fold with the conserved DxDD motif in the N-terminal half of the protein

TABLE 3 Inhibition of $WbwC_{ECO104}$ and $WbwC_{ECO5}$ activities[a]

Compound	Concn (mM)	% Inhibition of activity over control	
		$WbwC_{ECO104}$	$WbwC_{ECO5}$
N-butyryl-glucosamineβ-thio-2-naphthyl	0.5	<1	<1
N-butyryl-galactosamineα-benzyl	5.0	<1	<1
QT137, 1,4-bis-(3-methyl-1H-imidazolium-1-yl)butane dichloride	0.5	9.0	<1
QT139, 1,6-bis-(3-methyl-1H-imidazolium-1-yl)hexane dichloride	0.5	23.0	<1
QT136, 1,18-bis-(3-methyl-1H-imidazolium-1-yl)octadecane dichloride	0.5	24.1	55.2
QT135, 1,20-bis-(3-methyl-1H-imidazolium-1-yl)eicosane dichloride	0.5	87.8	97.5
QT148, 1,20-bis-(3-methyl-1H-imidazolium-1-yl)eicosane dimesylate	0.5	79.8	93.1
QT149, 1,22-bis-(3-methyl-1H-imidazolium-1-yl)docosane dimesylate	0.5	99.2	99.7

[a] WbwC assays were performed in duplicate determinations using purified enzymes as described in Materials and Methods. The acceptor concentration was 0.1 mM substrate 8.

(between amino acids 85 and 102). Most of these enzymes are inverting β1,3-glycosyltransferases, including β3Gal-transferases WbwC, WbbD, WbiP, WbgO, CgtB, LsgF, WbnJ, and Eps6 and the β1,3-Glc-transferases WbdN, WfaP, WfgD. In β3Gal-transferase WbiP from *E. coli*, the first and second Asp residues of the DxDD motif (Asp88 and Asp90) were mutated and suggested to be involved in UDP-Gal binding (37). Our study is the first to examine all three Asp residues of the DxDD motif. Interestingly, other enzymes of the GT2 family that are not β3-glycosyltransferases, e.g., β1,4-Gal- or β1,4-Glc-transferases, do not possess the DxDD motif. This suggests a functional importance of DxDD in the transfer of a Gal or Glc residue to position 3 of either GalNAc- or GlcNAc-containing acceptor substrates. We are awaiting the crystal structure of one of these enzymes in order to confirm the role of the DxDD motif in catalysis.

Another class of enzymes, the terpenoid cyclases, also have a conserved DxDD motif (43, 44). In these enzymes, the Asp residues are thought to cooperatively act as catalytic acids. The multiple Asp residues may thus enhance the ability of the catalytic Asp to protonate and in addition, in the terpenoid cyclases, are involved in binding the inhibitory metal ion Mg^{2+}.

The TF (or T) antigen has been recognized as an important tumor antigen that can be targeted for the clinical development of carbohydrate-based anticancer vaccines (16, 45). Various chemical strategies have been developed to synthesize TF antigen-containing glycopeptides (46). CgtB, a β1,3-Gal-transferase involved in the synthesis of the ganglioside-like Galβ1-3GalNAcβ linkage found in the lipooligosaccharides of *Campylobacter jejuni* (47), prefers the β linkage in the GalNAc-R acceptor but also acts on GalNAcα-R substrates and can synthesize the linkage of the TF antigen structure. WbiP also synthesizes the TF antigen, but direct proof using anti TF antibody has not been provided, although it is likely that anti-TF antigen antibodies bind the disaccharide Galβ1-3GalNAcα linked to a variety of structures, including oligosaccharides, peptides, and hydrophobic aglycones. We showed here that the TF antigen can also be linked to a diphosphate group. Thus, WbwC can be regarded as a T synthase (16, 17, 39) and may be useful for a chemoenzymatic synthesis of the TF antigen. The diphosphate group can easily be removed with pyrophosphatases and phosphatases to yield the reducing TF disaccharide that could further be linked to an aglycone group suitable for vaccine synthesis.

Human T synthase (core 1 β1,3-Gal-transferase, classified in the GT31 family of inverting glycosyltransferases), which synthesizes the TF antigen in mucin-type O-glycans, has minimal sequence identity with WbwC but may have a similar architecture at the catalytic site, which remains to be elucidated. In spite of similar properties of mammalian and bacterial Gal-transferases, it is interesting that human core 1 β1,3-Gal-transferase, which transfers Gal to GalNAcα-benzyl, does not accept GalNAcα-PP-PhU as a substrate and prefers peptide aglycones (39). In contrast, WbwC uses GalNAcα-PP-PhU as the acceptor but not GalNAcα-benzyl or GalNAcα-peptides. Another difference between the human and bacterial enzymes is the inhibition by bis-imidazolium salts that inhibit WbwC but not the human enzyme. In contrast, *N*-butyryl-galactosamine α-Bn inhibits only human T synthase and not WbwC.

Both $WbwC_{ECO104}$ and $WbwC_{ECO5}$ are specific for the axial 4-hydroxyl of the GalNAc and the diphosphate in the acceptor substrate. The requirement for the diphosphate linked to GalNAc or GlcNAc in the acceptors appears to be a characteristic of the second enzymes in the O antigen assembly pathways, which include WbwC (22–25, 48, 49). It is not known, however, if the α linkage of GalNAc is required and if both phosphate groups are necessary for high activity. Based on our experience, we expect that at least one phosphate residue directly linked to GalNAcα is an absolute requirement for WbwC, but this remains to be shown upon synthesis of the appropriate acceptor analogs (26, 50, 51). Previous studies showed that different lipid chains in the acceptor were compatible with high activities of Gal- and Glc-transferases (22, 24, 48). In the current study, we used two acceptors that differed in the terminal ring structure in the aglycone, suggesting that the structure of the lipid moiety may be of minor importance for *in vitro* activity. The acceptors may form micelles where GalNAc-PP is exposed while the lipid moiety is enclosed; this may mimic the *in vivo* Und-linked substrates that are embedded in the inner membrane.

There are two other putative glycosyltransferase genes in the *E. coli* O104-antigen gene cluster (*wbwA* and *wbwB*) that may encode the α2,3-NeuNAc-transferase and α1,4-Gal-transferase necessary to sequentially complete the assembly of the O104 repeating unit (18). WbwC can be used to synthesize the substrate for the next step in O104 antigen synthesis and to determine the functions of the enzymes encoded by the *wbwA* and *wbwB* genes. The *wzx* and *wzy* genes in the O104 gene cluster are expected to encode a flippase and polymerase, respectively (2, 18, 52, 53), which indicates that the O104 antigen biosynthesis is governed by the Wzy-polymerase-dependent pathway (8, 9, 52).

All of the bacterial enzymes characterized to date that assemble O antigens appeared to lack a transmembrane domain and prob-

ably reside close to the cytosolic face of the inner membrane with access to both the soluble nucleotide sugar pools and the membrane-bound Und substrates. Enzymes may be tethered to the membrane by a yet-unknown mechanism, possibly by an enzyme complex formation that maintains their high activity. In our *in vitro* assays of recombinant enzymes, this organization is lacking, explaining why these glycosyltransferases often show relatively low activity in the purified form. The acceptor substrate has detergent-like properties and may form micelles together with added detergents *in vitro*. The fact that the two WbwC enzymes differ in their response to detergents may be due to a characteristic recognition of substrates by the enzymes. The amino acid sequences of WbwC $_{ECO104}$ and WbwC $_{ECO104}$ differ by 47%, and different hydrophobic sequences may be exposed. However, the enzymes have very similar characteristics; thus, the amino acids essential for substrate binding and catalysis and the dimensions of the active sites may be identical in the two enzymes, which remains to be shown by protein structure analyses.

As the second enzyme in the O104 biosynthesis pathway, WbwC $_{ECO104}$ is a suitable target for blocking O104 antigen synthesis and thus reducing a virulence factor. The bis-imidazolium inhibitors are interesting drug candidates. Specific bis-imidazolium salts inhibit selected glycosyltransferases (8, 17) with IC_{50}s between 20 and 250 μM, while WbwC showed relatively low IC_{50}s of 8 to 18.6 μM. These inhibitors probably bind properly spaced negatively charged and hydrophobic patches on the enzyme and may distort protein structure or block either substrate binding or catalysis. Since bis-imidazolium salts inhibit only selected Gal-transferases, the mechanism of inhibition may not involve binding to negatively charged donor or acceptor substrates. Current investigations are aimed at elucidating the mode of inhibition *in vitro* and in bacteria.

Our present study shows the thorough characterization of two bacterial enzymes that synthesize a humanlike antigen. This work provides a possible biotechnology approach for the synthesis of functionally important bacterial and mammalian oligosaccharides.

ACKNOWLEDGMENTS

We thank Francoise Sauriol (Queen's University) for carrying out the NMR analyses and Jiaxi Wang for the mass spectra analyses (Queen's University). We thank Vladimir V. Veselovsky and his team at the Zelinsky Institute, Russian Academy of Sciences, Moscow, Russia, for the synthesis of the fluorescent substrate. We thank Kate Rittenhouse, Roswell Park Cancer Institute, Buffalo, NY, USA, for the anti-TF antibody and John Schutzbach for critically reading the manuscript.

This work was funded in part by a Discovery grant from the Natural Science and Engineering Research Council of Canada (to I.B.) and a grant from the Canadian Institutes of Health Research (to I.B. and W.A.S.), by a National 973 Program of China grant (2012CB721101), a National Natural Science Foundation of China (NSFC) Key Program grant (31030002), and the National Key Program for Infectious Diseases of China (2013ZX10004216-001-001) (to L.F.).

REFERENCES

1. **Ho TD, Waldor MK.** 2007. Enterohemorrhagic *Escherichia coli* O157:H7 Gal mutants are sensitive to bacteriophage P1 and defective in intestinal colonization. Infect. Immun. **75:**1661–1666. http://dx.doi.org/10.1128/IAI.01342-06.
2. **Raetz CR, Whitfield C.** 2002. Lipopolysaccharide endotoxins. Annu. Rev. Biochem. **71:**635–700. http://dx.doi.org/10.1146/annurev.biochem.71.110601.135414.
3. **Sheng H, Lim JY, Watkins MK, Minnich SA, Hovde CJ.** 2008. Characterization of an *Escherichia coli* O157:H7 O-antigen deletion mutant and effect of the deletion on bacterial persistence in the mouse intestine and colonization at the bovine terminal rectal mucosa. Appl. Environ. Microbiol. **74:**5015–5022. http://dx.doi.org/10.1128/AEM.00743-08.
4. **Strauss J, Burnham NA, Camesano TA.** 2009. Atomic force microscopy study of the role of LPS O-antigen on adhesion of *E. coli*. J. Mol. Recognit. **22:**347–355. http://dx.doi.org/10.1002/jmr.955.
5. **Zhang L, Radziejewska-Lebrecht J, Krajewska-Pietrasik D, Toivanen P, Skurnik M.** 1997. Molecular and chemical characterization of the lipopolysaccharide O-antigen and its role in the virulence of *Yersinia enterocolitica* serotype O8. Mol. Microbiol. **23:**63–76. http://dx.doi.org/10.1046/j.1365-2958.1997.1871558.x.
6. **Reeves PR, Hobbs M, Valvano MA, Skurnik M, Whitfield C, Coplin D, Kido N, Klena J, Maskell D, Raetz CR.** 1996. Bacterial polysaccharide synthesis and gene nomenclature. Trends Microbiol. **4:**495–503. http://dx.doi.org/10.1016/S0966-842X(97)82912-5.
7. **Shimizu T, Yamasaki S, Tsukamoto T, Takeda Y.** 1999. Analysis of the genes responsible for the O-antigen synthesis in enterohaemorrhagic *Escherichia coli* O157. Microb. Pathog. **26:**235–247. http://dx.doi.org/10.1006/mpat.1998.0253.
8. **Reeves PR.** 1994. Biosynthesis and assembly of lipopolysaccharide. New Comp. Biochem. **27:**281–314. http://dx.doi.org/10.1016/S0167-7306(08)60416-0.
9. **Whitfield C.** 1995. Biosynthesis of lipopolysaccharide O antigens. Trends Microbiol. **3:**178–185. http://dx.doi.org/10.1016/S0966-842X(00)88917-9.
10. **Qin J, Cui Y, Zhao X, Rohde H, Liang T, Wolters M, Li D, Belmar Campos C, Christner M, Song Y, Yang R.** 2011. Identification of the Shiga toxin-producing *Escherichia coli* O104:H4 strain responsible for a food poisoning outbreak in Germany by PCR. J. Clin. Microbiol. **49:**3439–3440. http://dx.doi.org/10.1128/JCM.01312-11.
11. **Creydt VP, Nuñez P, Boccoli J, Silberstein C, Zotta E, Goldstein J, Ibarra C.** 2006. Role of the Shiga toxin in the hemolytic uremic syndrome. Medicina (B. Aires) **66**(Suppl 3):S11–S15. (In Spanish.)
12. **Frank C, Werber D, Cramer JP, Askar M, Faber M, an der Heiden M, Bernard H, Fruth A, Prager R, Spode A, Wadl M, Zoufaly A, Jordan S, Kemper MJ, Follin P, Müller L, King LA, Rosner B, Buchholz U, Stark K, Krause G, Investigation Team HUS.** 2011. Epidemic profile of Shiga-toxin-producing *Escherichia coli* O104:H4 outbreak in Germany. N. Engl. J. Med. **365:**1771–1780. http://dx.doi.org/10.1056/NEJMoa1106483.
13. **Muniesa M, Hammerl JA, Hertwig S, Appel B, Brüssow H.** 2012. Shiga toxin-producing *Escherichia coli* O104:H4: a new challenge for microbiology. Appl. Environ. Microbiol. **78:**4065–4073. http://dx.doi.org/10.1128/AEM.00217-12.
14. **Gamian A, Romanowska E, Ulrich J, Defaye J.** 1992. The structure of the sialic acid-containing *Escherichia coli* O104 O-specific polysaccharide and its linkage to the core region in lipopolysaccharide. Carbohydr. Res. **236:**195–208. http://dx.doi.org/10.1016/0008-6215(92)85016-S.
15. **Urbina F, Nordmark EL, Yang Z, Weintraub A, Scheutz F, Widmalm G.** 2005. Structural elucidation of the O-antigenic polysaccharide from the enteroaggregative *Escherichia coli* strain 180/C3 and its immunochemical relationship with *E. coli* O5 and O65. Carbohydr. Res. **340:**645–650. http://dx.doi.org/10.1016/j.carres.2005.01.001.
16. **Brockhausen I, Gao Y.** 2012. Structural glycobiology, p 177–214. *In* Yuriev E, Ramsland PA (ed), Structural glycobiology: applications in cancer research. CRC Press, Taylor & Francis Group, Boca Raton, FL.
17. **Springer GF.** 1997. Immunoreactive T and Tn epitopes in cancer diagnosis, prognosis, and immunotherapy. J. Mol. Med. **75:**594–602. http://dx.doi.org/10.1007/s001090050144.
18. **Wang L, Briggs CE, Rothemund D, Fratamico P, Luchansky JB, Reeves PR.** 2001. Sequence of the *E. coli* O104 antigen gene cluster and identification of O104 specific genes. Gene **270:**231–236. http://dx.doi.org/10.1016/S0378-1119(01)00471-1.
19. **Rush JS, Alaimo C, Robbiani R, Wacker M, Waechter CJ.** 2010. A novel epimerase that converts GlcNAc-P-P-undecaprenol to GalNAc-P-P-undecaprenol in *Escherichia coli* O157. J. Biol. Chem. **285:**1671–1680. http://dx.doi.org/10.1074/jbc.M109.061630.
20. **Freinkman E, Chng SS, Kahne D.** 2011. The complex that inserts lipopolysaccharide into the bacterial outer membrane forms a two-protein plug-and-barrel. Proc. Natl. Acad. Sci. U. S. A. **108:**2486–2491. http://dx.doi.org/10.1073/pnas.1015617108.
21. **Wang L, Reeves PR.** 1998. Organization of *Escherichia coli* O157 O anti-

gen gene cluster and identification of its specific genes. Infect. Immun. **66:**3545–3551.
22. **Brockhausen I, Hu B, Liu B, Lau K, Szarek WA, Wang L, Feng L.** 2008. Characterization of two beta-1,3-glucosyltransferases from *Escherichia coli* serotypes O56 and O152. J. Bacteriol. **190:**4922–4932. http://dx.doi.org/10.1128/JB.00160-08.
23. **Gao Y, Liu B, Strum S, Schutzbach JS, Druzhinina TN, Utkina NS, Torgov VI, Danilov L, Veselovsky VV, Vlahakis JZ, Szarek WA, Wang L, Brockhausen I.** 2012. Biochemical characterization of WbdN, a beta1,3-glucosyltransferase involved in O-antigen synthesis in enterohemorrhagic *Escherichia coli* O157. Glycobiology **22:**1092–1102. http://dx.doi.org/10.1093/glycob/cws081.
24. **Riley JG, Menggad M, Montoya-Peleaz PJ, Szarek WA, Marolda CL, Valvano MA, Schutzbach JS, Brockhausen I.** 2005. The wbbD gene of *E. coli* strain VW187 (O7:K1) encodes a UDP-Gal: GlcNAc{alpha}-pyrophosphate-R {beta}1,3-galactosyltransferase involved in the biosynthesis of O7-specific lipopolysaccharide. Glycobiology **15:**605–613.
25. **Xu C, Liu B, Hu B, Han Y, Feng L, Allingham JS, Szarek WA, Wang L, Brockhausen I.** 2011. Biochemical characterization of UDP-Gal:GlcNAc-pyrophosphate-lipid β-1,4-Galactosyltransferase WfeD, a new enzyme from *Shigella boydii* type 14 that catalyzes the second step in O-antigen repeating-unit synthesis. J. Bacteriol. **193:**449–459. http://dx.doi.org/10.1128/JB.00737-10.
26. **Montoya-Peleaz PJ, Riley JG, Szarek WA, Valvano MA, Schutzbach JS, Brockhausen I.** 2005. Identification of a UDP-Gal:GlcNAc-R galactosyltransferase activity in *Escherichia coli* VW187. Bioorg. Med. Chem. Lett. **15:**1205–1211. http://dx.doi.org/10.1016/j.bmcl.2004.11.077.
27. **Vinnikova AN, Druzhinina TN, Danilov LL, Utkina NS, Torgov VI, Veselovsky VV, Wang S, Liu B, Wang L, Brockhausen I.** 2013. Synthesis of a fluorescent acceptor substrate for glycosyltransferases involved in the assembly of O-antigens of enterohemorrhagic *Escherichia coli* O157 and O5. Carbohydr. Res. **366:**17–24. http://dx.doi.org/10.1016/j.carres.2012.11.009.
28. **Brockhausen I, Benn M, Bhat S, Marone S, Riley JG, Montoya-Peleaz P, Vlahakis JZ, Paulsen H, Schutzbach JS, Szarek WA.** 2006. UDP-Gal: GlcNAc-R beta1,4-galactosyltransferase—a target enzyme for drug design. Acceptor specificity and inhibition of the enzyme. Glycoconj. J. **23:**525–541.
29. **Gao Y, Lazar C, Szarek WA, Brockhausen I.** 2010. Specificity of β1,4-galactosyltransferase inhibition by 2-naphthyl 2-butanamido-2-deoxy-1-thio-β-D-glucopyranoside. Glycoconj. J. **27:**673–684. http://dx.doi.org/10.1007/s10719-010-9312-3.
30. **Gao Y, Vinnikova A, Brockhausen I.** 2013. Functional identification of bacterial glucosyltransferase WbdN. Glycosyltransferases: methods and protocols in method molecular biology. Humana Press, Springer Science and Business Media, New York, NY.
31. **Gao Y, Vlahakis JZ, Szarek WA, Brockhausen I.** 2013. Selective inhibition of glycosyltransferases by bivalent imidazolium salts. Bioorg. Med. Chem. **21:**1305–1311. http://dx.doi.org/10.1016/j.bmc.2012.12.034.
32. **Visscher I, Stuart MC, Engberts JB.** 2006. The influence of phenyl and phenoxy modification in the hydrophobic tails of di-*n*-alkyl phosphate amphiphiles on aggregate morphology. Org. Biomol. Chem. **4:**707–712. http://dx.doi.org/10.1039/b514285g.
33. **Bernardes GJL, Kikkeri R, Maglinao M, Laurino P, Collot M, Hong SY, Lepenies B, Seeberger PH.** 2010. Design, synthesis and biological evaluation of carbohydrate-functionalized cyclodextrins and liposomes for hepatocyte-specific targeting. Org. Biomol. Chem. **8:**4987–4996. http://dx.doi.org/10.1039/c0ob00372g.
34. **Nakabayashi S, Warren CD, Jeanloz RW.** 1986. A new procedure for the preparation of oligosaccharide oxazolines. Carbohydr. Res. **150:**C7–C10. http://dx.doi.org/10.1016/0008-6215(86)80028-3.
35. **Fegan N, Barlow RS, Gobius KS.** 2006. *Escherichia coli* O157 somatic antigen is present in an isolate of *E. fergusonii*. Curr. Microbiol. **52:**482–486. http://dx.doi.org/10.1007/s00284-005-0447-6.
36. **Cheng J, Wang Q, Wang W, Wang Y, Wang L, Feng L.** 2006. Characterization of *E. coli* O24 and O56 O antigen gene clusters reveals a complex evolutionary history of the O24 gene cluster. Curr. Microbiol. **53:**470–476. http://dx.doi.org/10.1007/s00284-006-0032-7.
37. **Yi W, Perali RS, Eguchi H, Motari E, Woodward R, Wang PG.** 2008. Characterization of a bacterial β-1,3-galactosyltransferase with application in the synthesis of tumor-associated T-antigen mimics. Biochemistry **47:**1241–1248. http://dx.doi.org/10.1021/bi7020712.
38. **Liu XW, Xia C, Li L, Guan WY, Pettit N, Zhang HC, Chen M, Wang PG.** 2009. Characterization and synthetic application of a novel beta1,3-galactosyltransferase from *Escherichia coli* O55:H7. Bioorg. Med. Chem. **17:**4910–4915. http://dx.doi.org/10.1016/j.bmc.2009.06.005.
39. **Gao Y, Aryal RP, Ju T, Cummings Gahlay RDG, Jarvis DL, Matta KL, Vlahakis JZ, Szarek WA, Brockhausen I.** 2013. Acceptor specificities and selective inhibition of recombinant human Gal- and GlcNAc-transferases that synthesize core structures 1, 2, 3 and 4 of O-glycans. Biochim. Biophys. Acta **1830:**4274–4281. http://dx.doi.org/10.1016/j.bbagen.2013.04.001.
40. **Breton C, Snajdrová L, Jeanneau C, Koca J, Imberty A.** 2006. Structures and mechanisms of glycosyltransferases. Glycobiology **16:**29R–37R. http://dx.doi.org/10.1093/glycob/cwj016.
41. **Ünligil UM, Rini JM.** 2000. Glycosyltransferase structure and mechanism. Curr. Opin. Struct. Biol. **10:**510–517. http://dx.doi.org/10.1016/S0959-440X(00)00124-X.
42. **Liu B, Knirel YA, Feng L, Perepelov AV, Senchenkova SN, Wang Q, Reeves PR, Wang L.** 2008. Structure and genetics of *Shigella* O antigens. FEMS Microbiol. Rev. **32:**627–653. http://dx.doi.org/10.1111/j.1574-6976.2008.00114.x.
43. **Mann FM, Prisic S, Davenport EK, Determan MK, Coates RM, Peters RJ.** 2010. A single residue switch for Mg(2+)-dependent inhibition characterizes plant class II diterpene cyclases from primary and secondary metabolism. J. Biol. Chem. **285:**20558–20563. http://dx.doi.org/10.1074/jbc.M110.123307.
44. **Peters RJ, Croteau RB.** 2002. Abietadiene synthase catalysis: conserved residues involved in protonation-initiated cyclization of geranylgeranyl diphosphate to (+)-copalyl diphosphate. Biochemistry **41:**1836–1842. http://dx.doi.org/10.1021/bi011879d.
45. **Karsten U, Papsdorf G, Pauly A, Vojtesek B, Moll R, Lane EB, Clausen H, Stosiek P, Kasper M.** 1993. Subtypes of non-transformed human mammary epithelial cells cultured in vitro: histo-blood group antigen H type 2 defines basal cell-derived cells. Differentiation **54:**55–56. http://dx.doi.org/10.1111/j.1432-0436.1993.tb01588.x.
46. **Brocke C, Kunz H.** 2002. Synthesis of tumor-associated glycopeptide antigens. Bioorg. Med. Chem. **10:**3085–3112. http://dx.doi.org/10.1016/S0968-0896(02)00135-9.
47. **Bernatchez S, Gilbert M, Blanchard M-C, Karwaski M-F, Li J, DeFrees S, Wakarchuk WW.** 2007. Variants of the β1,3-galactosyltransferase CgtB from the bacterium *Campylobacter jejuni* have distinct acceptor specificities. Glycobiology **17:**1333–1343. http://dx.doi.org/10.1093/glycob/cwm090.
48. **Brockhausen I, Riley JG, Joynt M, Yang X, Szarek WA.** 2008. Acceptor substrate specificity of UDP-Gal:GlcNAc-R β1,3-galactosyltransferase (WbbD) from *Escherichia coli* O7:K1. Glycoconj. J. **25:**663–673. http://dx.doi.org/10.1007/s10719-008-9127-7.
49. **Yi W, Yao Q, Zhang Y, Motari E, Lin S, Wang PG.** 2006. The *wbnH* gene of *Escherichia coli* O86:H2 encodes an α-1,3-N-acetylgalactosaminyl transferase involved in the O-repeating unit biosynthesis. Biochem. Biophys. Res. Commun. **344:**631–639. http://dx.doi.org/10.1016/j.bbrc.2006.03.181.
50. **Brockhausen I, Larsson EA, Hindsgaul O.** 2008. A very simple synthesis of GlcNAc-alpha-pyrophosphoryl-decanol: a substrate for the assay of a bacterial galactosyltransferase. Bioorg. Med. Chem. Lett. **18:**804–807. http://dx.doi.org/10.1016/j.bmcl.2007.11.031.
51. **Riley JG, Xu C, Brockhausen I.** 2010. Synthesis of acceptor substrate analogs for the study of glycosyltransferases involved in the second step of the biosynthesis of O-antigen repeating units. Carbohydr. Res. **345:**586–597. http://dx.doi.org/10.1016/j.carres.2009.12.022.
52. **Samuel G, Reeves P.** 2003. Biosynthesis of O-antigens: genes and pathways involved in nucleotide sugar precursor synthesis and O-antigen assembly. Carbohydr. Res. **338:**2503–2519. http://dx.doi.org/10.1016/j.carres.2003.07.009.
53. **Valvano MA.** 2003. Export of O-specific lipopolysaccharide. Front. Biosci. **8:**s452–s471. http://dx.doi.org/10.2741/1079.